Water Research X 12 (2021) 100105

Contents lists available at ScienceDirect

Water Research X

journal homepage: www.sciencedirect.com/journal/water-research-x

UV aged epoxy coatings– Ecotoxicological effects and released compounds

Anna Maria Bell, Nils Keltsch, Peter Schweyen, Georg Reifferscheid, Thomas Ternes, Sebastian Buchinger *

Federal Institute of Hydrology, Am Mainzer Tor 1, 56068 Koblenz, Germany

ARTICLE INFO

Keywords:
Epoxide
Leaching
Toxicity
UV-A
Effect-directed analysis

ABSTRACT

Organic coatings can guarantee long-term protection of steel structures due to causing a physical barrier against water and oxygen. Because of their mechanical properties and resistances to heat and chemicals, epoxy resin-based coatings are widely used for corrosion protection. Despite of the aromatic backbone and the resulting susceptibility to UV degradation, epoxy resins are frequently used as binding agent in top layers of anti-corrosion coating systems. Consequently, these organic polymers are directly exposed to sunlight and thus UV radiation. The present study was designed to investigate if toxic effects of epoxy resin-based-coatings are changed by UV-A irradiation. For this purpose, two epoxide-based top coatings were examined with and without UV aging for their bacterial toxicity and estrogenicity. In addition, chemical analyses were performed to identify released compounds as well as photolytic degradation products and to assign toxic effects to individual substances. UV-A irradiation of epoxy resin based top coatings resulted in an overall decrease of acute and specific ecotoxicological effects but as well to the formation of toxic transformation products. Both, in leachates of untreated and UV-A irradiated coatings, 4*t*BP was identified as the main driver of estrogenicity and toxicity to luminescent bacteria. BPA and structural analogs contributing to estrogenic effects in leachates were formed by UV-A irradiation. The combination of HPTLC coupled bioassays and LC-MS analyses supported the identification of bioactive compounds in terms of an effect-directed analysis. The present findings indicate that epoxide-based coatings are less suitable for the application as top coatings and more UV stable coatings like aliphatic polyurethanes should be preferred.

Introduction

Alterations of metallic (construction) materials by the reaction with their environment are summarized under the term corrosion. To maintain relevant infrastructures, this natural process can be prevented by active and passive protection methods. Active corrosion protection is done by the negative polarization of the steel e. g. by galvanic anodes or impressed-current systems. In contrast, passive protection methods achieve their anti-corrosive properties by acting as barrier between the metal and the corrosive environment. An effective and frequently used passive method is the application of organic coatings systems since they can provide long-term protection of steel structures even under aggressive environmental conditions (e.g. in industrial or marine applications). Besides major steel structures such as bridges, (offshore) wind turbines and buildings, the bodyworks of vehicles are protected by organic coatings (Lyon et al. 2017). Protective paint systems are designed for protection periods up to over 25 years and are internationally standardized according to ISO 12944-1 (ISO 2018a). In perspective, systems even providing at least 50 years of corrosion protection are intended to be approved (Kuhlmann 2020).

For the fabrication of organic coatings, a wide range of binding agents can be applied, such as alkyd resins, acrylic resins, ethyl silicates, fluoropolymers, polyester resins, polysiloxanes, polyacrylates and polyaspartates (ISO 2018a). The most commonly used coatings are based on polyurethane or epoxy resins. A complete anti-corrosion coating system can consist of up to three different coating layers (priming, intermediate and top coating), which themselves consisting of one or two components and are applied usually in up to 360 μm film thickness. After application, the coating is continually exposed to weathering, especially to UV radiation. Because of their aromatic backbone, epoxide-based coatings have a decreased UV-stability compared to coatings based on polyurethane. Nevertheless, the former is frequently used as top layers in anti-corrosion coating systems. Consequently, these organic polymers are irradiated by sunlight and thus UV radiation. This might trigger the

* Corresponding author at: Federal Institute of Hydrology, Department G3 - Biochemistry, Ecotoxicology, Am Mainzer Tor 1, 56068 Koblenz, Germany.
E-mail address: Buchinger@bafg.de (S. Buchinger).

https://doi.org/10.1016/j.wroa.2021.100105
Received 29 March 2021; Received in revised form 26 May 2021; Accepted 27 May 2021
Available online 2 June 2021

degradation of the chemical structure of the coating caused by the cleavage of chemical bonds due to photolysis and the attack of free radicals (autoxidation) (Hare 1992). Besides the negative effects on the durability of the coating by e.g. cracking or delamination from the coated surface, the light-induced degradation could possibly lead to the formation of transformation products with unwanted biological activities.

Depending on the corrosive category and protection period, the resistance of paints to weathering is examined as part of their performance testing under artificial (cycle test according to ISO 12944) and natural conditions (long-term exposure in nature according to BAW (2011)). The ISO standard asks for reduced emissions of volatile organic compounds (VOC) and prohibits the use of toxic and carcinogenic ingredients, but the assessment of possible environmental impacts is not part of the authorization of corrosion protection systems. However, coatings based on epoxy resins can contain a wide range of organic solvents, metallic pigments, UV stabilizers, biocides, and other potential hazardous substances as bisphenol A/F, alkylphenols and other phenolic substances and polyamines, which are added as curing agents (Jin et al. 2015, Verma et al. 2020). All these ingredients and reaction products formed during the hardening by polyaddition reactions potentially pose a risk to the aquatic environment if released from respective steel structures either by a direct contact with a water body or indirectly via the runoff from the structure after rainfall.

In previous studies the leaching of bisphenol A, nonylphenol and 4-*tert*-butylphenol from various unweathered epoxy resin-based coatings was already reported. In this context, estrogenic activity and toxic effects to water fleas, luminescent bacteria and cypris larvae of barnacles were detected (Bell et al. 2020, Vermeirssen et al. 2017, Watermann et al. 2005). In contrast, investigations on UV aged coatings were mainly focused on topics of material and polymer sciences such as the mechanisms of photodegradation or structural and performance changes. For instance, Liu et al. (2014) studied the microstructural alteration of a polyamide-cured epoxy coating and discovered the formation of micropores along with an increased water barrier function upon UV-A irradiation. Brand et al. (2020) recently investigated irradiated coating surfaces and elucidated degradation pathways leading to the delamination of polyurethane top layers. However, the toxicity of UV aged coatings to the (aquatic) environment has not been addressed so far.

Therefore, this study was designed to investigate if toxic effects of epoxy resin-based-coatings are changed by UV-A irradiation. For this purpose, two epoxide-based top coatings were examined with and without UV aging for their bacterial toxicity and estrogenicity. In addition, chemical analyses were performed to identify released compounds as well as photolytic products and to assign toxic effects to individual substances.

Material and methods

Selection of coating systems and fabrication of test plates

The current study was performed with two different two-component epoxide-based top coatings for corrosion protection known for their elevated bacterial toxicity and estrogenic effects from previous investigations (Bell et al. 2020). The selected products are primarily used for the corrosion protection of hydraulic steel structures and are among the most relevant coatings for the federal transport infrastructure of Germany. The coating was performed by the Institute for Corrosion Protection (IKS, Dresden). The respective layers were applied on the front, back and edges of steel plates with a size of 150×160×3 mm following the respective instructions provided by the manufacturer of the coatings. The particular layer thickness was defined by the list of approved coating systems of the BAW and amounted to 200 μm and 500 μm for coating A and B, respectively.

The treatment with UV-A radiation was conducted in an indoor UV-chamber (UVA CUBE 400, Dr. Hönle AG, Germany) for 65 h only on the front of the coated plates with an average power of 230 W/m^2 and a total energy amount of 53.82 MJ/m^2. The UV doses were recorded using the corresponding UV-Meter equipped with an optical fiber sensor (340-405 nm). Using 215 MJ/m^2 as reference annual UV-radiation dose in central Europe (295-400 nm) (Atlas Material Testing Solutions 2001), the released radiation is equivalent to approximately three months of real time exposure in central Europe (230 W/m^2 × 65 h × 3600 s/h = 53.82×10^6 J/m^2).

Leaching and sample preparation

The coated plates were attached on nylon strings and immersed in 3 l deionized water filled into all-glass aquariums (300×220×240 mm). The containers were covered by glass plates. Leaching water was sampled after 4 weeks and stored in closed, dark glass bottles at 2 to 8°C. Samples that were not examined within 48 h after collection were kept frozen at ≤ −18°C until further analysis. An aliquot of each sample was concentrated 1000-fold by solid phase extraction (SPE) using OASIS HLB 6cc (200mg) cartridges. The selected sorbent is designed for a universal application and can retain a wide range of acidic, basic, and neutral substances. The cartridges were conditioned with 2 ml n-heptane (Picograde, Promochem), 2 ml acetone (Picograde, Promochem), 3 × 2 ml methanol (Optigrade, Promochem) and 4 × 2 ml double distilled water and then loaded with 1000 ml of the aqueous samples. After drying, the SPE cartridges were eluted with 4 × 2 ml methanol. Extracts were evaporated and restored in ethanol (Optigrade, Promochem). Each coating was investigated as triplicate with and without UV aging. Two aquaria without plates served as controls.

Bioassays

Luminescent bacteria assay

The bioluminescence of the marine bacterium *Aliivibrio fischeri* can be utilized to assess acute bacterial toxicity by quantifying the inhibition of the bacterial light emission after exposure to the test sample.

Luminescent bacteria assay in 96-well plates. The procedure of bioluminescence inhibition assay in 96-well plates was adapted from DIN EN ISO 11348-2 (ISO 2007) and performed with reconstituted liquid-dried bacteria (LCK 482, Hach Lange). Prior testing, ethanolic extracts were pre-diluted at least 1→1000 and simultaneously salinated with NaCl solution (2 %, m/v). Each sample was tested in dilution series in a geometric sequence, three-fold independently in white 96-well microtiter plates (μCLEAR, Greiner Bio-One) with three technical replicates each. Together with the three independent leaching experiments, nine biologically independent tests were performed in total for each coating and condition (with/without UV). A NaCl solution (2 %, m/v) was used as negative control and 3,5-dichlorophenol (97 %, Sigma; c = 4.5 mg/l) served as positive control. The half maximal effect concentration in terms of sample dilution (EC50) calculated from the tested dilution series was used as test result.

HPTLC coupled luminescent bacteria assay. For the performance of the HPTLC coupled luminescent bacteria assay, liquid-dried bacteria were reactivated with 4 ml of supplied reactivation solution and cultivated in 200 ml liquid medium for pre- and main cultures according to DIN EN ISO 11348-1 (ISO 2007b) in an Erlenmeyer flask with cap under constant agitation (350 ± 50 rpm) for 48 ± 2 h at room temperature. On the day of analysis, ethanolic extracts were sprayed in 5 mm bands using the automatic TLC sampler ATS 4 (Camag) on a HPTLC plate (Silica gel 60 F_{254} glass plates, 20×10 cm, Merck Chemicals, prewashed with Methanol and activated by drying for 30 min at 110°C). Chromatographic development was conducted in the automated developing chamber AMD 2 (Camag) with ethyl acetate (Optigrade, Promochem) and

n-hexane (Lichrosolv, Merck) (35:65, v/v) after focusing the samples with methanol. Before exposition with luminescent bacteria, the solvents on the plates were allowed to evaporate for at least 3 h. Subsequently, the plates were dipped into a suspension of luminescent bacteria with the Chromatogram Immersion Device 3 (Camag) for 1 s at highest speed. The supernatant suspension was removed from the silica surface using a squeegee. The bioluminescence was documented after an exposure time of 11 min by using a cooled 16 bit CCD camera integrated in the BioLuminizer (Camag). Toxic fractions appear as dark zones.

Yeast estrogen screen (YES)

The reporter gene assay is based on the activation of the human estrogen receptor alpha (ERα) in case of the presence of ERα-agonists in the sample. The activation of the receptor is measured by a reporter gene assay using the *lacZ*-gene - encoding the enzyme β-galactosidase - as the reporting element. The applied test strain according to McDonnell et al. (1991b) (1991a) is based on the strain *Saccharomyces cerevisiae* BJ3505 (protease deficient, MATα, PEP4::HIS3, prb-1-δ1.6R, HIS3-δ200, lys2-801, trp1-δ101, ura3-52gal2can1).

Yeast estrogen screen in 96-well plates. The estrogenicity was investigated in 96-well microtiter plates (Cellstar, Greiner Bio-One) according to ISO 19040-1 (ISO 2018b) by exposing the genetically modified yeast cells at 30°C for 18 h to dilutions of the ethanolic extracts. Each sample was tested at least three-fold independently with four technical replicates each. Together with the three independent leaching experiments, nine biologically independent tests were performed for each coating and condition (with/without UV). Single compounds were investigated at least three times independently. Ethanol (1 %) was used as negative control and a dilution series of 17β-estradiol (E2) (≥ 98 %, Sigma-Aldrich) served as positive control (500 – 0.66 ng/l) and for calibration. The estrogenic potential of samples was quantified in terms of a 17β-estradiol equivalent concentration (EEQ).

HPTLC coupled yeast estrogen screen (p-YES). The investigation of estrogen-like effects on HPTLC-plates was performed according to Riegraf et al. (2019) and the chromatographic procedure was adopted from the luminescent bacteria assay (see 2.3.1.2). The yeast cells were exposed to the plates by spraying and incubated for 3 h under saturated humid atmosphere (NuAire CO_2-incubator with humidity control, NU-5820E). Estrogenic fractions appearing as fluorescent zones were documented using a TLC Visualizer 2 (CAMAG) at an excitation wavelength of 366 nm.

Data evaluation and statistics

The statistical analysis of bioassay data was performed using the open source software R (version 3.4.3). The fits of concentration-response relationships and estimates of EC50 were generated by a five-parameter log-logistic function (equation 1) by means of the extension package drc (version 3.0.1).

$$f(x) = c + \frac{d - c}{(1 + \exp(b \times (\log(x) - \log(e))))^f} \quad (1)$$

The response of respective bioassays was evaluated as a function of concentration x with the parameters c and d as lower and upper response limits, respectively. The parameter e is defined as inflection point, parameter b denotes the relative slope and the parameter f describes the asymmetry of the curve.

Toxic units were calculated by dividing the mass concentrations of quantified standards (see Table 2) by their respective half maximal effective concentration (EC50) of the single compounds determined by the characterization of a complete concentration-response relationship in the YES and luminescent bacteria assay in 96-well plates.

Chemical analyses

Qualitative and quantitative analysis of extracts

The identification and quantification of compounds released from untreated and UV-A aged coating systems were performed with an HPLC system (1260 Infinity series, Agilent Technology, Waldbronn, Germany) coupled to a high resolution mass spectrometer (TripleTOF, AB SCIEX). The QTOF system was equipped with a DuoSpray ion source and a TuboIon Spray probe for electro spray ionization (ESI) experiments. The parameter for positive and negative ionization were as follows (values for ESI(-) in parenthesis): ion source gas (GS) 1 and 2: 35 and 45 psi; curtain gas (CUR): 40 psi; source temperature (TEM): 550°C; ion spray voltage floating (ISVF): 5500 eV (-4500 ev), declustering potential (DP): 60 V (-100 V); ion release delay (IRD): 67 ms; ion release width (IRW): 25 ms. Full scan experiments (100-1200 Da) were performed with an accumulation time of 0.2 s in the high sensitivity mode. Eight independent data acquisition (IDA) experiments were acquired for MS^2 spectra accumulation (accumulation time: 0.05 s). The fragmentation conditions were as follows: mass range: 30-1200 Da; CE: 40 eV (-40 eV), collision energy spread (CES): 15 eV (-15 eV). The mass spectrometer was automatically re-calibrated after four runs using an automated calibrant delivery system (CDS) via atmospheric pressure chemical ionization (APCI). Chromatographic separation by HPLC was performed on a Zorbax Eclipse Plus C18 column (Narrow Bore RR, 2.1 × 150 mm, 5 μm) with a Zorbax Eclipse XDB-C8 Guard column (2.1 × 12.5 mm, 5 μm), both obtained from Agilent. The eluent depends on the polarity of the measurement. For positive ionization a gradient elution with Milli-Q water (A) and methanol (B), both with 0.1 % formic acid, was performed. Because of an insufficient ionization for some analytes in the positive ionization mode, the detection was performed as well in the negative ionization mode using a gradient elution with Milli-Q water (A2) and methanol (B2) without adding formic acid. The following solvent gradient with a flow rate of the mobile phase of 0.3 ml/min was applied for both measurements: 0-2 min, 30 % B (B2); 2-4 min, 80 % B (B2); 4-12 min, 98 % B (B2); 12-16 min, 98 % B (B2); 16-20 min, 30 % B (B2); 20-25 min, 30 % B (B2). The injection volume was 10 μl and the column temperature was set to 50°C. MS data acquisition was controlled with Analyst 1.6.2 (SCIEX). For the quantification of target compounds (Table 1) an external 9-point calibration was performed ranging from 10 to 250,000 ng/l in methanol. The identity of each analyte in the samples was checked by comparing retention time, high resolution MS^1 and high resolution MS^2 fragmentation of the corresponding $[M+H]^+$ or $[M-H]^-$ against the respective authentic standard. The response area of $[M+H]^+$ respectively $[M-H]^-$ at MS^1 level was used for quantification. Data processing was performed by the software MultiQuantTM 3.0.2 (SCIEX). The samples were measured after dilution with methanol by a dilution factor of 1×10^{-2}, 1×10^{-4} or 2×10^{-6} to reach the linear calibration range.

Effect-directed analysis of bioactive fractions

The identification of compounds contributing to bacterial toxicity and estrogen-like effects of the extracts was performed by thin layer chromatography. The extracts were developed according to the proceeding in HPTLC coupled assays. Based on the previously detected bioactive zones, toxic fractions were marked on the surface of the HPTLC plate with a pencil. The silica layer was scraped off the glass at relevant positions with a scalpel and placed in a reaction tube. The obtained fractions were extracted with 500 μl ethanol (Optigrade, Promochem) by thoroughly mixing for 30 s. After the centrifugation of the suspensions for 1 min at 14,000 *g*, the supernatants were filtered (PTFE, 0.45 μm) and subjected to LC-MS analysis as described in section 2.4.1.

Table 1
Analytical parameters of target compounds. Quantification limits (LOQ) are given at the level of the lowest analyte concentration of the calibration. Ionization mode used for quantification is indicated by underlining the respective precursor ion mass.

substance	CAS	retention time	theoretical mass (m/z)		LOQ
		[min]	$[M+H]^+$	$[M-H]^-$	[mg/l]
4-*tert*-butylphenol (4*t*BP) 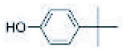	98-54-4	7.40	151.112	<u>149.097</u>	1.25
bisphenol A (BPA) 	80-05-7	6.85	229.122	<u>227.108</u>	0.63
4-cumylphenol (4CP) 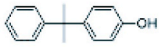	599-64-4	6.53	245.117	<u>243.102</u>	0.03
4-[1-(4-methoxyphenyl)-1-methylethyl]phenol (BPA-I11) 	16530-58-8	7.86	243.138	<u>241.123</u>	0.13
5-hydroxybisphenol A (BPA-I10) 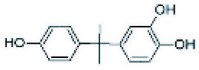	79371-66-7	8.03	213.127	<u>211.112</u>	0.63
bisphenol A diglycidyl ether 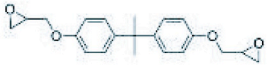	1675-54-3	7.97	<u>341.175</u>	339.160	1.25
bisphenol A (2,3-dihydroxypropyl) glycidyl ether 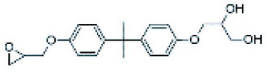	76002-91-0	7.19	<u>359.185</u>	357.171	1.25
bisphenol A bis(2,3-dihydroxypropyl) ether (Bis-HPPP) 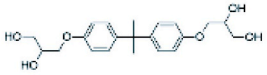	5581-32-8	6.67	<u>377.196</u>	375.181	0.13
bisphenol F 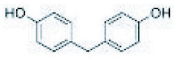	620-92-8	6.43	201.091	<u>199.076</u>	0.63
2-phenylphenol (2PP) 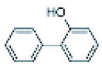	90-43-7	7.22	171.080	<u>169.066</u>	0.13
4-nonylphenol 	104-40-5	11.04	221.190	<u>219.175</u>	1.25

Results

Alteration of toxicity by UV irradiation

In order to investigate, if ecotoxicological effects of epoxide-based coatings are changed by UV-A irradiation, two different top coatings were examined with and without UV-aging for their bacterial toxicity and estrogenicity.

All tested leachates caused high toxicity to bacteria and induced estrogenic effects. Interestingly, the UV-A irradiation of the coatings resulted in a significant decrease of toxicological effects (see Figure 1). In total, 185 ± 19 ng/l EEQ were determined in leachates of coating A without UV aging, whereas the mean EEQ concentration was 152 ± 13 ng/l in the corresponding leachates of UV aged coatings. The leachates of coating B contained 50.6 ± 7.2 ng/l EEQ without UV aging and 31.4 ± 4.5 ng/l EEQ after UV-irradiation. In the bioluminescence inhibition assay, the EC50-values in terms of percentage of the sample in the assay of coating A and B without UV aging were 0.190 ± 0.002 % and 0.820 ± 0.011 %, respectively. The UV-A irradiated plates resulted in EC50-values of 0.260 ± 0.002 % in case of coating A and 1.860 ± 0.031 % in case of coating B.

Formation of toxic transformation products

Despite the observed reduced toxicity caused by the UV aging of coatings, it cannot be excluded that bioactive transformation products (TPs) are formed during the treatment and released into the environment. HPTLC coupled bioassays can assist in the identification of toxic compounds by the determination of toxic fractions in continuously separated samples. Therefore, leachates of untreated and UV-A irradiated coatings were investigated for differences in effect patterns by means of the HPTLC coupled luminescent bacteria assay as well as the planar Yeast Estrogen Screen (p-YES). The bioactive HPTLC fractions of respective standards and selected samples were subsequently analyzed by LC/MS. The phenols 4*t*BP and BPA were suspected targets to be present as bioactive compounds due to their identification in previous studies investigating leachates of coatings for corrosion protection.

In all leachates of coatings without UV aging, bacterial toxicity was observed as only one, very intense signal at a Rf-value of 0.74 (see Figure 2A and Figure SI 2A). At the same height a signal with less intensity was detected in all leachates of coatings with UV aging. In case of the irradiated coating an additional inhibition zone occurred at a Rf-value of 0.32. All signals showed a dose dependent variation of intensity (see Figure SI 3). The same effect patterns were observed by the p-YES (see Figure 2B and Figure SI 2B) with the difference that minimal estrogenic activity already becomes visible at a Rf-value of 0.32 in leachates of coatings without UV aging. However, the increased signal intensity after UV-irradiation at Rf = 0.32 is clearly evident.

The Rf-values of observed effect signals matched well with the pattern of the suspected compounds 4*t*BP and BPA (not shown). The subsequent comparison of chromatograms revealed the presence 4*t*BP at a Rf-value of 0.74 and BPA at a Rf-value of 0.32 (Figure 3).

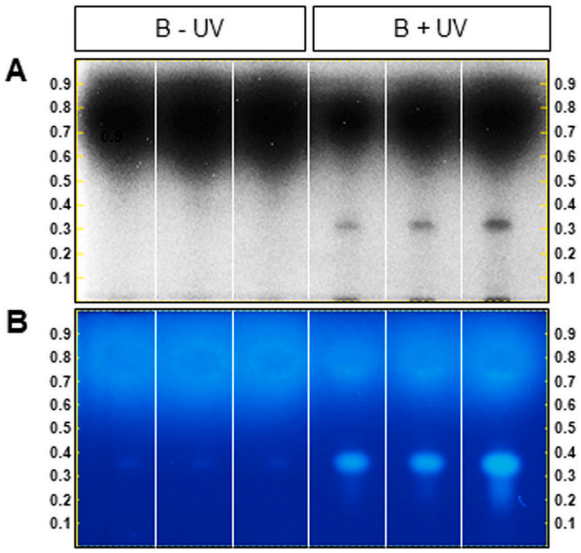

Fig. 2. Toxicity in leachates of untreated (- UV) and UV-A irradiated (+ UV) coating B on HPTLC-plate. The ethanolic extracts (1000-fold concentrated) of all replicates were chromatographically developed with ethyl acetate / n-hexane (35:65). For a better visualization brightness and contrast were adjusted. *A*: Black and white image of luminescence signals after 11 min exposure of luminescent bacteria. The 1:10 diluted extracts were applied in a volume of 10 µl each. *B*: Fluorescence image of HPTLC coupled Yeast Estrogen Screen at an excitation wavelength of 366 nm. The 1:10 diluted extracts were applied in a volume of 5 µl each.

Released substances

Following the initial identification, the samples were further analyzed for possible transformation products of BPA and other phenolic compounds by a targeted LC-tandem MS-approach. In addition to 4*t*BP and BPA, further four phenols, namely 4-cumylphenol (4CP), 4-[1-(4-methoxyphenyl)-1-methylethyl]phenol (BPA-I11), 5-hydroxybisphenol A (BPA-I10), bisphenol A bis(2,3-dihydroxypropyl) ether (Bis-HPPP), and 2-phenylphenol (2PP) were identified. These compounds were subsequently quantified by an external calibration (see Table 2). Three of these substances (4*t*BP, BPA and Bis-HPPP) were detected in all samples, further three (4CP, BPA-I11, BPA-I10) only in leachates of UV-irradiated coatings and one (2PP) just in leachates of untreated coating B. The contents of 4*t*BP and Bis-HPPP were significantly lower in leachates of UV-irradiated coatings compared to leachates of coating without UV treatment. The release of 4*t*BP was reduced by around 40 % and 45 % in leachates of coating A and B, respectively, leachates of UV-irradiated coating A showed a release of Bis-HPPP reduced on average by 72 % compared to the untreated coating A. In contrast, in leachates of

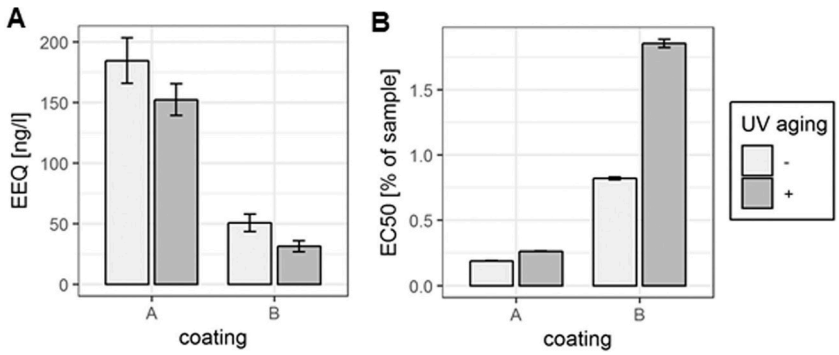

Fig. 1. Toxic effects in leachates of untreated (-) and UV-A irradiated (+) coatings A and B (mean, n = 9, error bars indicate SE). Experiments were performed with concentrated samples. The presented results are calculated for the original aqueous leachates. Negative controls showed no effects. For the full dose-response data see Figure SI 1. *A*: Estrogenic activities detected as estradiol-equivalents (EEQ) with a recombinant yeast estrogen screen. *B*: Toxicity to luminescent bacteria is shown as EC50.

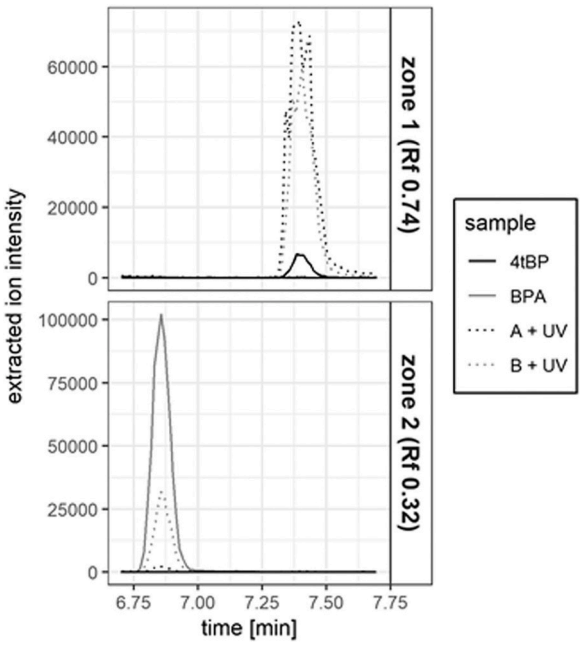

Fig. 3. Extracted ion chromatograms of mass-to-charge ratio 227.108 (representing BPA) and 149.097 (representing 4*t*BP). Selected samples of UV-A irradiated coatings A and B as well as standard solutions of 4*t*BP and BPA were chromatographically developed on HPTLC plate with ethyl acetate and n-hexane (35:65). Toxic fractions were extracted and analyzed by LC-MS.

UV-irradiated coatings A and B the concentration of BPA increased about 6 and 19 times compared to leachates of coatings without UV-treatment.

Characterization of effects caused by identified compounds

In addition to the quantification of the released substances, the individual compounds were characterized regarding to their toxic potency using the HPTLC-coupled and the microplate bioassays. On basis of the latter test approach, the relative contribution of individual substances to the bacterial toxicity and estrogen-like effects were estimated.

All the substances quantified in the leachates of the coatings were toxic to luminescent bacteria (Figure SI 5A). By far the highest toxicity was observed in the presence of 4*t*BP (EC50 = 14.0 ± 0.4 µg/l), which was also detected in the highest concentrations in the leachates. Therefore, the toxicity to luminescent bacteria was virtually completely driven by 4*t*BP and the contribution of the other quantified substances is negligible.

Six of the seven quantified substances showed estrogenic effects (Figure SI 5B). In this context, the most potent substance was 4CP (EC50 = 44.9 ± 5.9 µg/l) followed by BPA-I11 (EC50 = 161.3 ± 1.8 µg/l) and BPA (EC50 = 302 ± 24 µg/l). Although 4*t*BP induced the estrogenic effects less strong (EC50 = 6300 ± 220 µg/l), it could explain more than 99 % of the estrogenicity of discovered compounds in leachates of untreated coatings (see Figure 4). Likewise, in leachates of UV irradiated coatings the estrogenic effects were driven by 4*t*BP, the mean contribution to estrogenicity of the quantified substances in leachates of coating A and B was 97 % and 81 %, respectively. On average, BPA explained 3 % and 16 % of the overall estrogenic potential caused by the identified compounds in samples of UV irradiated coatings A and B. In leachates of UV irradiated coating B, 2 % and 1 % of the estrogenicity can be assigned to BPA-I11 and 4CP, respectively. Although BPA-I10 and 2PP showed estrogenic potential in single testing, they did not contribute to the observed effects due to their low concentrations in the leachates. Bis-HPPP was not estrogenic far above the measured concentrations.

The investigation of single standards with the HPTLC coupled assays has shown that 4CP and 2PP are potentially contributing to the intense effect signals at Rf-value of 0.74 (Figure SI 4). Moreover, in appropriate concentrations the substances BPA-I11 and BPA-I10 become visible as additional signals at Rf-value of 0.62 and 0.05, respectively.

Discussion

The investigation of two epoxy resin based top coatings revealed the potential release of hazardous substances into the environment along with elevated toxicity to luminescent bacteria and estrogen-like effects (see Table SI 1). Similar results were obtained in a study by Vermeirssen et al. (2017) who investigated leachates of anonymized epoxy resin based anti-corrosion coatings and detected up to 280 ng/l EEQ under worst case conditions. In contrast to the present observations, BPA and not 4*t*BP was identified as the main driver for the estrogenic effect in concentrations up to 10.4 mg/l BPA. In the luminescence inhibition assay, the lowest EC50 was determined by Vermeirssen et al. at a sample concentration of 0.4 %. This finding is in the range of the results reported in the current study.

The observed decrease of ecotoxicological effects in leachates of UV-A irradiated coatings can be associated with the significant decrease of 4*t*BP concentrations. A volatilization of 4*t*BP during the fabrication of test plates could be responsible for this reduction. The treatment with UV-A radiation leads to increased temperatures of the investigated coating materials and thus an elevated evaporation of 4*t*BP is likely. Secondly, a possible degradation of 4*t*BP to less or non-toxic substances might explain reduced concentrations of 4*t*BP and lower toxic effects. Previous studies identified 4-(2-methyl-2-propanyl)-2-[4-(2-methyl-2-propanyl)phenoxy]phenol, 4,4′-di-*tert*-butyl-o,o'-biphenol, 4-*tert*-butylcatechol and 2-*tert*-butylphenol as TPs of 4*t*BP that can be generated by UV photolysis (Cirkva et al. 2005, Wu et al. 2016). To the best of our knowledge, for the two first mentioned TPs no analytical standards are available and ecotoxicological effects are not documented so far. In contrast, the 4*t*BP-degradation product 4-*tert*-butylcatechol is

Table 2
Quantified target compounds (n = 3, SE = standard error of the mean) in leachates of untreated (- UV) and UV-A irradiated (+ UV) coatings A and B. Compounds were measured after a 1000-fold enrichment, the results refer to the original aqueous samples under the assumption of a quantitative extraction of the compounds. Abbreviations of substances see Table 1. The measured concentrations in corresponding blank controls were below the quantification limit.

coating	4*t*BP [µg/l]		BPA [µg/l]		4CP [µg/l]		BPA-I11 [µg/l]		BPA-I10 [µg/l]		Bis-HPPP [µg/l]		2PP [µg/l]	
	mean	SE	mean	SE	mean	SE	mean	SE	mean	SE	mean	SE	mean	SE
A - UV	15000	1400	2.30	0.10	< LOQ		< LOQ		< LOQ		19.6	1.1	< LOQ	
A + UV	9400	2000	14.3	1.6	< LOQ		0.72	0.16	0.78	0.06	5.6	2.7	< LOQ	
B - UV	3320	110	0.90	0.01	< LOQ		< LOQ		< LOQ		1.04	0.40	0.67	0.23
B + UV	1840	410	16.9	3.7	0.23	0.17	1.37	0.48	1.20	0.23	0.95	0.20	< LOQ	

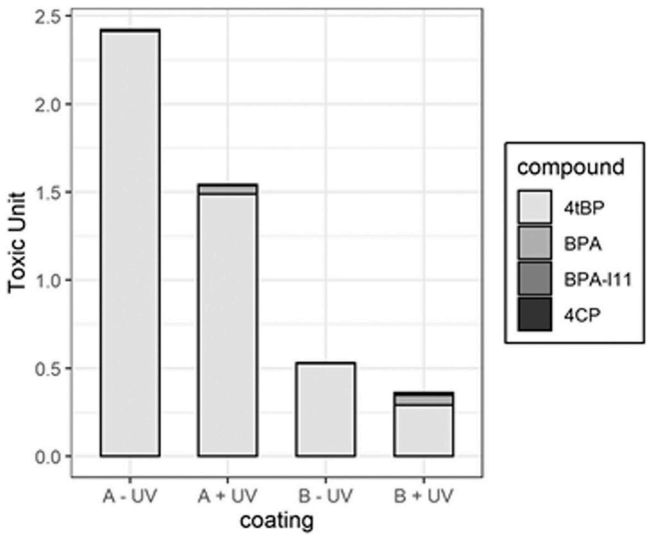

Fig. 4. Toxic units (c/EC50) of main compounds contributing to estrogenic effects in leachates of untreated (- UV) and UV-A irradiated (+ UV) coatings A and B. The estimates of EC50 were generated by a five-parameter log-logistic function (equation 1). Bis-HPPP, BPA-I10 and 2PP had no significant contribution to the estrogenic potential caused by the identified compounds and are therefore not displayed.

categorized as very toxic to aquatic life and the European Chemicals Agency (ECHA) proposes a predicted no effect concentration (PNEC) of 1.2 μg/l for freshwater. For 2-*tert*-butylphenol various endocrine effects were documented. For example, Tollefsen and Nilsen (2008) determined the binding affinity of 2-*tert*-butylphenol to the hepatic estrogen receptor from rainbow trout. Li et al. (2010) demonstrated antagonistic effects to the androgen receptor and gamma inverse agonistic effects to an estrogen-related receptor using a set of recombined yeast strains.

In contrast to the reduced release of 4*t*BP, the release of BPA from both coatings was increased by the UV-A irradiation . BPA is the basis of the most common epoxy resins as it is a major compound for the production of the resin monomer, bisphenol A diglycidyl ether (BADGE). During the curing of coating components, the monomers are crosslinked by polyaddition reactions with polyfunctional amines added as hardener. Earlier studies demonstrated that the photooxidative change of epoxy polymers can be caused by various mechanisms. The UV radiation of epoxy resins e.g. can lead to a chain scission of C–N bonds and ring opening reactions of oxirane groups (Brand et al. 2020, Kim and Urban 2000, Liu et al. 2014). This indicates that respective parts of the polymeric matrix were degraded and/or released into the environment. BPA is one of the world's most important and commonly produced industrial chemicals. It primarily serves as intermediate in the production of polycarbonate and epoxy resins. Furthermore, it is used as additive e.g. in the manufacture of thermal paper, tires and flame retardants. Due to its widespread use, BPA has been found in waters since the late 1990s and is now detectable in almost all environmental compartments (Corrales et al. 2015, Michalowicz 2014). In particular, the input of BPA into the environment can be related to traffic and the release from construction materials. Lamprea et al. (2018) investigated a representative selection of building materials and automotive supplies and identified lacquered car bodyworks as important source of BPA contamination in urban runoff with a tested water emission of up to 360 ng/cm^2. On this basis, it can be assumed that the emission of BPA from weathered coatings plays a significant role in the overall exposure. However, investigations on a larger scale or, ideally, a substance flow analysis for BPA would be necessary for a robust estimation of the contribution to the overall pollution. In a European Union Risk Assessment Report dating from 2010, monitoring data for BPA in European water bodies were published; a mean concentration of 0.13 μg/l for freshwaters and 60 ng/g dry weight for freshwater sediments was reported (EC 2010). BPA is recognized as endocrine disruptor, can have adverse effects on the immune system and liver, promotes mutagenesis and carcinogenesis and is supposed to mediate neurotoxic and teratogenic effects (Michalowicz 2014). The ECHA proposes a PNEC of 18 μg/l in freshwaters and 1.2 μg/g dry weight in freshwater sediments.

Besides BPA, four related compounds could be identified via LC-MS analyses. Three of them (BPA-I10, 4CP and BPA-I11) were only detected in leachates of UV-irradiated coatings and were therefore assumed to be photolytic degradation products of BPA or the BPA based polymer. In aqueous solution, the degradation reaction of UV irradiated BPA followed a pseudo-first-order kinetic with a half-life time about 6 h (Kovacic et al. 2019). The light sensitivity of BPA and the formation of a variety of derivates by photochemical processes were already reported in former studies (Cardoso da Silva et al. 2014, Im and Loffler 2016, Kondrakov et al. 2014, Molkenthin et al. 2013). In this context, BPA-I10 was formerly identified as photo-transformation product of BPA. So far, to the best of our knowledge, the occurrence of BPA-I10 in environmental samples was not reported. The competitive binding of BPA-I10 to ERα was reported with a half maximal inhibition concentration (IC50) of 50 μM and at the same time this transformation product was identified as slightly less potent than BPA (IC50 = 10 μM) (Nakagawa and Suzuki 2001). In toxicity testing with MCF-7 and NIH3T3 cells, BPA-I10 exhibited estrogen-like and anti-androgenic effects with an EC50 of 1.8 μM and 14 μM, respectively (Kitamura et al. 2005). The present results of the yeast estrogen screen (EC50 = 7.5 mg/l or 31 μM) lie in the range of the previous reports. Moreover, Mutou et al. (2006) demonstrated a cytotoxicity of BPA-I10 on Jurkat cells in concentrations from 5 to 50 μM (1.2 to 12 mg/l). This amounts to the same order of magnitude as the present results of acute bacterial toxicity.

4CP is known as impurity in industrial grade BPA (Terasaki et al. 2004) and is used as an intermediate for the production of phenolic resins, insecticides and lubricants. In Polish surface waters, concentrations up to 6.2 ng/l were detected (Czarczynska-Goslinska et al. 2017). Further monitoring data for 4CP is mainly available for Asia ranging from about 2 ng/l in river estuaries around Dianchi Lake in China (Wang et al. 2013) up to 160 ng/l in river water of Nagoya city in Japan (Hasegawa et al. 2016). Moreover, investigations at the Panlong River in China revealed sediment concentrations up to 4.8 ng/g and a bioconcentration factor (BCF) of up to 10 by analyzing muscle, liver and gill tissue of wild fish (Wang et al. 2016). In one of six muscle samples of freshwater prawn from local supermarkets in USA, 4CP could also be detected with 1.96 ng/g wet weight (Zuo and Zhu 2014). Perez-Albaladejo et al. (2019) reported that 4CP induced cytotoxic effects (EC50 = 65 μM), led to the generation of reactive oxygen species (2–3-fold at 50 μM) and increased the P450 aromatase activity (1.3-fold at 20 μM) in human placental JEG-3 cells. In a yeast two-hybrid assay, 4CP showed 12 times higher estrogenic effects than BPA (Terasaki et al. 2005). This observation is consistent with the present data revealing a nearly 7 times lower EC50 of 4CP compared to BPA. Furthermore, a recent study reported that low concentrations of 4CP and BPA induce the proliferation of MCF-7 cells synergistically (Wang et al. 2020). Investigations of Rosenmai et al. (2014) indicate that 4CP act by several modes of action within the endocrine system. For example, the activation of estrogen receptor (EC50 = 0.10 μM) and the inhibition of the androgen receptor (EC50 = 5.1 μM) was determined by reporter gene assays. Furthermore, agonistic effects on the retinoic acid (RA) receptor (1.68 μM 4CP showed 20% of the activity of 0.1 μM all-trans RA) were shown (Kamata et al. 2008). A PNEC of 14.2 μg/l and 3.58 μg/g dry weight is proposed by the ECHA for freshwater and freshwater sediments.

BPA-I11 was previously mentioned as product of microbial transformation (McCormick et al. 2011) and of photodegradation catalyzed by nano TiO_2 (Jia et al. 2012). Information on the occurrence of BPA-I11 in environmental samples is very limited. Ashfaq et al. (2018) determined an average concentration of 2.75 ng/l in Jiulong River, China.

Investigations on the competitive binding to ERα as well as the gene induction and cell proliferation with MCF-7 cells exhibited BPA-I11 as less estrogenic than BPA (Coleman et al. 2003). For instance, the relative effect on proliferation in response to BPA-I11 and BPA differed by one order of magnitude (2.63×10^{-4} vs. 2.00×10^{-3}, EC50 relative to estradiol). The opposite trend was observed during the present study, as compared by EC50 the effected estrogenicity of BPA-I11 was approximately twice as high as the effect induced by BPA. Furthermore, BPA-I11 was found to be responsible for the disruption of mitosis and cytokinesis in HeLa cells by inducing the formation of ectopic spindle poles (George et al. 2008). Even if the correlation of aneuploidy and tumorigenesis is not fully understood, this result indicates that BPA-I11 can exhibit carcinogenic effects. McCormick et al. (2011) reported a half maximal lethal concentration of up to 0.66 mg/l BPA-I11 to zebrafish embryos and thus an almost eight times higher toxicity as BPA.

The present study indicates that the UV aging of epoxy coatings could contribute to the emission of BPA and its transformation products into the environment. Due to the potentially incomplete enrichment of hazardous substances by SPE, the actual toxicity might even be underestimated. If a release may lead to locally elevated concentrations and pose an environmental risk, needs to be further investigated in field and laboratory studies. So far, known environmental concentrations are all below the proposed PNECs. However, the information on the environmental fate and effects of the TPs is very limited and PNECs were defined only for individual substances. As two of the identified photolytic products, i.e. 4CP and BPA-I11, are found to be more potent in the YES and the luminescent bacteria assay than BPA itself, they could be of more serious concern especially if continuously released and/or accumulated. The present study investigated changes in toxicity caused by approximately three months of real time exposure to sunlight. To explore the underlying degradation and release kinetics and to predict the total environmental impact of photodegradation products, the individual protection period of coatings (up to 25 years) has to be considered. For a more complete picture also further weathering parameters (e.g. temperature, humidity and precipitation) and coating materials should be investigated.

Compared to other materials such as polyurethanes, acrylics, polyesters or alkyds, epoxy resins are well known for their susceptibility to UV degradation (Knudsen and Forsgren 2017). The absorption of UV radiation by aromatic moieties can lead to the breakdown of the polymeric structure along with the discoloration and chalking of the coating layer (Ghasemi-Kahrizsangi et al. 2015). To compensate this disadvantage, epoxy resin-based coatings are frequently covered by top coatings based on polyurethane. Furthermore, the UV resistance of polymers can be improved by different additives as light screens, UV absorbers, radical scavengers or quenchers (Hawkins 1984). Recent studies demonstrated that the UV resistance of epoxy coatings can for example be enhanced by polyaniline nanowires (Gao et al., 2021) or TiO_2 nanoparticles blended with poly-dimethylamino siloxane (Fadl et al. 2020). To extend the service life of steel coatings and to reduce their emissions in outdoor exposure to solar radiation, it is advisable to adjust the recipe of UV sensitive coatings accordingly or to use top layers with more photostable binding agents.

Conclusion

- The susceptibility of epoxy resin-based coatings to UV degradation was demonstrated by the alteration of acute and specific ecotoxicological effects and the release of toxic transformation products.
- Both, in leachates of untreated and UV-A irradiated coatings, 4*t*BP was identified as the main driver of estrogenicity and toxicity to luminescent bacteria. Additionally, BPA and close structural analogs contribute to estrogenic effects in leachates of UV-A irradiated materials.
- The combination of HPTLC coupled bioassays and LC-MS analyses supported the identification of bioactive compounds in terms of an effect-directed analysis.
- Due to their lower UV-stability compared to e.g. polyurethanes, epoxy resin-based coatings are less suitable for the application as top coatings.

Declaration of competing interest

The authors declare that they have no known competing financial interests or personal relationships that could have appeared to influence the work reported in this paper.

Acknowledgement

The authors thank Marina Ohlig for the preparation of extracts and the support in performing the HPTLC coupled luminescent bacteria assay and the planar Yeast Estrogen Screen, Ramona Pfänder for technical assistance with the Yeast Estrogen Screen and Ames fluctuation test, Christel Möhlenkamp for the pre-analyses of samples by GC-MS and Simon Brand for UV treatment of the test plates.

This study was funded by the German Federal Ministry of Transport and Digital Infrastructure (BMVI) in the context of the BMVI Network of Experts.

Supplementary materials

Supplementary material associated with this article can be found, in the online version, at doi:10.1016/j.wroa.2021.100105.

References

Ashfaq, M., Sun, Q., Zhang, H., Li, Y., Wang, Y.W., Li, M.Y., Lv, M., Liao, X., Yu, C.P., 2018. Occurrence and fate of bisphenol A transformation products, bisphenol A monomethyl ether and bisphenol A dimethyl ether, in wastewater treatment plants and surface water. J. Hazard. Mater. 357, 401–407. https://doi.org/10.1016/j.jhazmat.2018.06.022.

Atlas Material Testing Solutions (2001) Weathering Testing Guidebook. http://www.strenometer.dk/Files/Downloads/Guidebook.pdf.

BAW (2011) Prüfung von Beschichtungssystemen für den Korrosionsschutz im Stahlwasserbau (RPB). [Guidelines for the testing of coating systems for the corrosion protection of hydraulic steel structures].

Bell, A.M., Baier, R., Kocher, B., Reifferscheid, G., Buchinger, S., Ternes, T., 2020. Ecotoxicological characterization of emissions from steel coatings in contact with water. Water Res. 173, 13. https://doi.org/10.1016/j.watres.2020.115525.

Brand, S., Veith, L., Baier, R., Dietrich, C., Schmid, M.J., Ternes, T.A., 2020. New methodical approaches for the investigation of weathered epoxy resins used for corrosion protection of steel constructions. J. Hazard. Mater. 395, 122289 https://doi.org/10.1016/j.jhazmat.2020.122289.

Cardoso da Silva, J.C., Reis Teodoro, J.A., de Cassia Franco Afonso, R.J., Aquino, S.F., Augusti, R., 2014. Photodegradation of bisphenol A in aqueous medium: Monitoring and identification of by-products by liquid chromatography coupled to high-resolution mass spectrometry. Rapid Commun. Mass Spectrom. 28 (9), 987–994. https://doi.org/10.1002/rcm.6863.

Cirkva, V., Kurfurstova, J., Karban, J., Hajek, M., 2005. Microwave photochemistry III: Photochemistry of 4-tert-butylphenol. J. Photochem. Photobiol. a-Chem. 174 (1), 38–44. https://doi.org/10.1016/j.jphotochem.2005.03.004.

Coleman, K.P., Toscano, W.A., Wiese, T.E., 2003. QSAR models of the in vitro estrogen activity of bisphenol A analogs. QSAR Comb. Sci. 22 (1), 78–88. https://doi.org/10.1002/qsar.200390008.

Corrales, J., Kristofco, L.A., Steele, W.B., Yates, B.S., Breed, C.S., Williams, E.S., Brooks, B.W., 2015. Global Assessment of Bisphenol A in the Environment: Review and Analysis of Its Occurrence and Bioaccumulation. Dose-Response 13 (3), 29. https://doi.org/10.1177/1559325815598308.

Czarczynska-Goslinska, B., Zgoia-Grzeskowiak, A., Jeszka-Skowron, M., Frankowski, R., Grzeskowiak, T., 2017. Detection of bisphenol A, cumylphenol and parabens in surface waters of Greater Poland Voivodeship. J. Environ. Manage. 204, 50–60. https://doi.org/10.1016/j.jenvman.2017.08.034.

EC (2010) Updated European Union Risk Assessment Report, 4, 4′-Isopropylidenediphenol (Bisphenol-A): environment addendum of February 2008. doi:10.2788/40195.

Fadl, A.M., Abdou, M.I., Hamza, M.A., Sadeek, S.A., 2020. Corrosion-inhibiting, self-healing, mechanical-resistant, chemically and UV stable PDMAS/TiO2 epoxy hybrid nanocomposite coating for steel petroleum tanker trucks. Prog. Org. Coat. 146, 20. https://doi.org/10.1016/j.porgcoat.2020.105715.

Gao, M., Wang, J.X., Cong, C., Ma, C.H., Morshed, M., Wang, Z., 2021. Degradation of epoxy coatings cooperated with polyaniline nanowires in the outdoor environment. Polym. Adv. Technol. 12. https://doi.org/10.1002/pat.5146.

George, O., Bryant, B.K., Chinnasamy, R., Corona, C., Arterburn, J.B., Shuster, C.B., 2008. Bisphenol A directly targets tubulin to disrupt spindle organization in embryonic and somatic cells. ACS Chem. Biol. 3 (3), 167–179. https://doi.org/10.1021/cb700210u.

Ghasemi-Kahrizsangi, A., Neshati, J., Shariatpanahi, H., Akbarinezhad, E., 2015. Improving the UV degradation resistance of epoxy coatings using modified carbon black nanoparticles. Prog. Org. Coat. 85, 199–207. https://doi.org/10.1016/j.porgcoat.2015.04.011.

Hare, C.H., 1992. The degradation of coatings by ultraviolet light and electromagnetic radiation. J. Protect. Coat. Linings.

Hasegawa, H., Hirao, S., Suzuki, S., 2016. Liquid Chromatography-mass Spectrometric Analysisof p-cumylphenol and Bisphenol A in Environmental Waters in Nagoya City. 環境化学 26 (1), 21–26. https://doi.org/10.5985/jec.26.21.

Hawkins, W.L., 1984. Polymer Degradation and Stabilization. Spinger Berlin Heidelberg.

Im, J., Loffler, F.E., 2016. Fate of Bisphenol A in Terrestrial and Aquatic Environments. Environ. Sci. Technol. 50 (16), 8403–8416. https://doi.org/10.1021/acs.est.6b00877.

ISO (2007) Water quality - Determination of the inhibitory effect of water samples on the light emission of Vibrio fischeri (Luminescent bacteria test) - Part 2: Method using liquid-dried bacteria.

ISO (2018a) Paints and varnishes - Corrosion protection of steel structures by protective paint systems.

ISO (2018b) Water quality - Determination of the estrogenic potential of water and waste water - Part 1: Yeast estrogen screen (Saccharomyces cerevisiae).

Jia, C.Z., Wang, Y.X., Zhang, C.X., Qin, Q.Y., Kong, S.Q., Yao, S.K., 2012. Photocatalytic Degradation of Bisphenol A in Aqueous Suspensions of Titanium Dioxide. Environ. Eng. Sci. 29 (7), 630–637. https://doi.org/10.1089/ees.2011.0132.

Jin, F.L., Li, X., Park, S.J., 2015. Synthesis and application of epoxy resins: A review. J. Ind. Eng. Chem. 29, 1–11. https://doi.org/10.1016/j.jiec.2015.03.026.

Kamata, R., Shiraishi, F., Nishikawa, J.I., Yonemoto, J., Shiraishi, H., 2008. Screening and detection of the in vitro agonistic activity of xenobiotics on the retinoic acid receptor. Toxicol. in Vitro 22 (4), 1050–1061. https://doi.org/10.1016/j.tiv.2008.01.002.

Kim, H., Urban, M.W., 2000. Molecular level chain scission mechanisms of epoxy and urethane polymeric films exposed to UV/H2O. Multidimensional spectroscopic studies. Langmuir 16 (12), 5382–5390. https://doi.org/10.1021/la990619i.

Kitamura, S., Suzuki, T., Sanoh, S., Kohta, R., Jinno, N., Sugihara, K., Yoshihara, S., Fujimoto, N., Watanabe, H., Ohta, S., 2005. Comparative study of the endocrine-disrupting activity of bisphenol A and 19 related compounds. Toxicol. Sci. 84 (2), 249–259. https://doi.org/10.1093/toxsci/kfi074.

Knudsen, O.Ø., Forsgren, A., 2017. Corrosion Control Through Organic Coatings. CRC Press.

Kondrakov, A.O., Ignatev, A.N., Frimmel, F.H., Brase, S., Horn, H., Revelsky, A.I., 2014. Formation of genotoxic quinones during bisphenol A degradation by TiO2 photocatalysis and UV photolysis: a comparative study. Appl. Catal. B-Environ. 160, 106–114. https://doi.org/10.1016/j.apcatb.2014.05.007.

Kovacic, A., Cesen, M., Laimou-Geraniou, M., Lambropoulou, D., Kosjek, T., Heath, D., Heath, E, 2019. Stability, biological treatment and UV photolysis of 18 bisphenols under laboratory conditions. Environ. Res. 179, 11. https://doi.org/10.1016/j.envres.2019.108738.

Kuhlmann, U., 2020. Stahlbau Kalender 2020: Schwerpunkte: Neue Normung im Hochbau; Leichtbau [Steel construction calendar 2020: Focus: New standards in building construction; Lightweight construction]. Wiley.

Lamprea, K., Bressy, A., Mirande-Bret, C., Caupos, E., Gromaire, M.C., 2018. Alkylphenol and bisphenol A contamination of urban runoff: an evaluation of the emission potentials of various construction materials and automotive supplies. Environ. Sci. Pollut. Res. 25 (22), 21887–21900. https://doi.org/10.1007/s11356-018-2272-z.

Li, J., Ma, M., Wang, Z.J., 2010. In vitro profiling of endocrine disrupting effects of phenols. Toxicol. in Vitro 24 (1), 201–207. https://doi.org/10.1016/j.tiv.2009.09.008.

Liu, F.W., Yin, M.X., Xiong, B.Y., Zheng, F., Mao, W.F., Chen, Z., He, C.Q., Zhao, X.P., Fang, P.F., 2014. Evolution of microstructure of epoxy coating during UV degradation progress studied by slow positron annihilation spectroscopy and electrochemical impedance spectroscopy. Electrochim. Acta 133, 283–293. https://doi.org/10.1016/j.electacta.2014.04.002.

Lyon, S.B., Bingham, R., Mills, D.J., 2017. Advances in corrosion protection by organic coatings: What we know and what we would like to know. Prog. Org. Coat. 102, 2–7. https://doi.org/10.1016/j.porgcoat.2016.04.030.

McCormick, J.M., Van Es, T., Cooper, K.R., White, L.A., Haggblom, M.M., 2011. Microbially Mediated O-Methylation of Bisphenol a Results in Metabolites with Increased Toxicity to the Developing Zebrafish (Danio rerio) Embryo. Environ. Sci. Technol. 45 (15), 6567–6574. https://doi.org/10.1021/es200588w.

McDonnell, D., Nawaz, Z., Densmore, C., Weigel, N., Pham, T., Clark, J., O'Malley, B, 1991a. High level expression of biologically active estrogen receptor in Saccharomyces cerevisiae. J. Steroid Biochem. Mol. Biol. 39 (3), 291–297. https://doi.org/10.1016/0960-0760(91)90038-7.

McDonnell, D.P., Nawaz, Z., O'Malley, B.W, 1991b. In situ distinction between steroid receptor binding and transactivation at a target gene. Mol. Cell. Biol. 11 (9), 4350–4355. https://doi.org/10.1128/mcb.11.9.4350.

Michalowicz, J., 2014. Bisphenol A - Sources, toxicity and biotransformation. Environ. Toxicol. Pharmacol. 37 (2), 738–758. https://doi.org/10.1016/j.etap.2014.02.003.

Molkenthin, M., Olmez-Hanci, T., Jekel, M.R., Arslan-Alaton, I., 2013. Photo-Fenton-like treatment of BPA: Effect of UV light source and water matrix on toxicity and transformation products. Water Res. 47 (14), 5052–5064. https://doi.org/10.1016/j.watres.2013.05.051.

Mutou, Y., Ibuki, Y., Terao, Y., Kojima, S., Goto, R., 2006. Chemical change of chlorinated bisphenol A by ultraviolet irradiation and cytotoxicity of their products on Jurkat cells. Environ. Toxicol. Pharmacol. 21 (3), 283–289. https://doi.org/10.1016/j.etap.2005.09.005.

Nakagawa, Y., Suzuki, T., 2001. Metabolism of bisphenol A in isolated rat hepatocytes and oestrogenic activity of a hydroxylated metabolite in MCF-7 human breast cancer cells. Xenobiotica 31 (3), 113–123. https://doi.org/10.1080/00498250110040501.

Perez-Albaladejo, E., Lacorte, S., Porte, C., 2019. Differential Toxicity of Alkylphenols in JEG-3 Human Placental Cells: Alteration of P450 Aromatase and Cell Lipid Composition. Toxicol. Sci. 167 (2), 336–346. https://doi.org/10.1093/toxsci/kfy243.

Riegraf, C., Reifferscheid, G., Belkin, S., Moscovici, L., Shakibai, D., Hollert, H., Buchinger, S., 2019. Combination of yeast-based in vitro screens with high-performance thin-layer chromatography as a novel tool for the detection of hormonal and dioxin-like compounds. Anal. Chim. Acta 1081, 218–230. https://doi.org/10.1016/j.aca.2019.07.018.

Rosenmai, A.K., Dybdahl, M., Pedersen, M., van Vugt-Lussenburg, B.M.A., Wedebye, E. B., Taxvig, C., Vinggaard, A.M., 2014. Are Structural Analogues to Bisphenol A Safe Alternatives? Toxicol. Sci. 139 (1), 35–47. https://doi.org/10.1093/toxsci/kfu030.

Terasaki, M., Nomachi, M., Edmonds, J.S., Morita, M., 2004. Impurities in industrial grade 4,4 '-isopropylidene diphenol (bisphenol A): possible implications for estrogenic activity. Chemosphere 55 (6), 927–931. https://doi.org/10.1016/j.chemosphere.2003.11.063.

Terasaki, M., Shiraishi, F., Nishikawa, T., Edmonds, J.S., Morita, M., Makino, M., 2005. Estrogenic activity of impurities in industrial grade bisphenol A. Environ. Sci. Technol. 39 (10), 3703–3707. https://doi.org/10.1021/es048932g.

Tollefsen, K.E., Nilsen, A.J., 2008. Binding of alkylphenols and alkylated non-phenolics to rainbow trout (Oncorhynchus mykiss) hepatic estrogen receptors. Ecotoxicol. Environ. Saf. 69 (2), 163–172. https://doi.org/10.1016/j.ecoenv.2007.04.010.

Verma, C., Olasunkanmi, L.O., Akpan, E.D., Quraishi, M.A., Dagdag, O., El Gouri, M., Sherif, E.S.M., Ebenso, E.E, 2020. Epoxy resins as anticorrosive polymeric materials: A review. React. Funct. Polym. 156, 20. https://doi.org/10.1016/j.reactfunctpolym.2020.104741.

Vermeirssen, E.L.M., Dietschweiler, C., Werner, I., Burkhardt, M, 2017. Corrosion protection products as a source of bisphenol A and toxicity to the aquatic environment. Water Res. 123, 586–593. https://doi.org/10.1016/j.watres.2017.07.006.

Wang, B., Dong, F.Q., Chen, S., Chen, M.J., Bai, Y.C., Tan, J.Y., Li, F.C., Wang, Q., 2016. Phenolic endocrine disrupting chemicals in an urban receiving river (Panlong river) of Yunnan-Guizhou plateau: Occurrence, bioaccumulation and sources. Ecotoxicol. Environ. Saf. 128, 133–142. https://doi.org/10.1016/j.ecoenv.2016.02.018.

Wang, B., Huang, B., Jin, W., Zhao, S.M., Li, F.R., Hu, P., Pan, X.J., 2013. Occurrence, distribution, and sources of six phenolic endocrine disrupting chemicals in the 22 river estuaries around Dianchi Lake in China. Environ. Sci. Pollut. Res. 20 (5), 3185–3194. https://doi.org/10.1007/s11356-012-1236-y.

Wang, X.X., Luo, N., Xu, Z.X., Zheng, X.Y., Huang, B., Pan, X.J., 2020. The estrogenic proliferative effects of two alkylphenols and a preliminary mechanism exploration in MCF-7 breast cancer cells. Environ. Toxicol. 35 (5), 628–638. https://doi.org/10.1002/tox.22898.

Watermann, B., Daehne, B., Sievers, S., Dannenberg, R., Overbeke, J., Klijnstra, J., Heemken, O.J.C, 2005. Bioassays and selected chemical analysis of biocide-free antifouling coatings. Chemosphere 60 (11), 1530–1541. https://doi.org/10.1016/j.chemosphere.2005.02.066.

Wu, Y.L., Shi, J., Chen, H.C., Zhao, J.F., Dong, W.B., 2016. Aqueous photodegradation of 4-tert-butylphenol: by-products, degradation pathway and theoretical calculation assessment. Sci. Total Environ. 566, 86–92. https://doi.org/10.1016/j.scitotenv.2016.05.064.

Zuo, Y.G., Zhu, Z., 2014. Simultaneous identification and quantification of 4-cumyl-phenol, 2,4-bis-(dimethylbenzyl)phenol and bisphenol A in prawn Macrobrachium rosenbergii. Chemosphere 107, 447–453. https://doi.org/10.1016/j.chemosphere.2014.01.058.